

# Discovery of a Featureless X-Ray Spectrum in the Supernova Remnant Shell of G330.2+1.0

Ken'ichi TORII, Hiroyuki UCHIDA, Kazuto HASUIKE, and Hiroshi TSUNEMI  
*Department of Earth and Space Science, Graduate School of Science, Osaka University*  
1-1 Machikaneyama-cho, Toyonaka, Osaka 560-0043  
Yasuhiro YAMAGUCHI and Shinpei SHIBATA  
*Department of Physics, Yamagata University,*  
Kojirakawa, Yamagata, Yamagata 990-8560

(Received 2005 October 30; accepted 2005 December 16)

## Abstract

We report here on the first pointed X-ray observation of the supernova remnant (SNR) G330.2+1.0. The X-ray morphology is characterized by an extended shell. Its X-ray spectrum is well represented by a single power-law function with a photon index of  $\gamma \simeq 2.8$  and interstellar absorption of  $n_{\text{H}} \simeq 2.6 \times 10^{22} [\text{cm}^{-2}]$ . We interpret this emission as synchrotron radiation from accelerated electrons at the SNR shock, as seen in SN 1006. The surface brightness of the X-ray emission is anti-correlated with the radio emission, and the power-law spectrum is dominated at the western shell where the radio emission is weak. The co-existence of two distinct (radio bright/X-ray faint and radio faint/X-ray bright) shells in a single supernova remnant challenges our understanding of the particle acceleration and radiation mechanisms in different interstellar environments. The object may be a good target for searching TeV gamma-rays and molecular gas surrounding the blast shock. We also report on the nature of a bright point-like source (AX J1601–5143) to the south of the SNR.

**Key words:** ISM: supernova remnants — acceleration of particles — X-rays: individual (G330.2+1.0)

## 1. Introduction

Our understanding of the origin and the acceleration mechanism of cosmic-ray particles has been a great challenge in astrophysics since the last century. X-ray observations have revealed that acceleration is taking place in supernova remnant shells by detecting featureless power-law type spectra (Koyama et al. 1995; Koyama et al. 1997; Slane et al. 2001). These spectra are interpreted as synchrotron radiation from accelerated electrons. The detections of TeV photons in RX J1713.7–3946 (Muraishi et al. 2000; Aharonian et al. 2004) and RX J0852.0–4622 (Aharonian et al. 2005) have assured the presence of high-energy (>TeV) particles, either leptons or hadrons, in these SNR shells.

The radio source of G330.2+1.0 is characterized by a clumpy distorted shell of 11' diameter (Caswell et al. 1983; Whiteoak, Green 1996). Caswell et al. (1983) attributed its morphology as being due to the interaction of a shock wave with a dense medium, particularly toward the lower galactic latitude (southeast). A clumpiness in the radio map led Whiteoak and Green (1996) to classify G330.2+1.0 as a possible composite type. As we show in the following sections, there is no signature of a Crab-like, compact X-ray source at the position of the clumpy radio shell. We therefore classify G330.2+1.0 as a shell type.

The HI absorption spectrum to the SNR gives a minimum kinematic distance of  $4.9 \pm 0.3$  kpc, while the greater distance for velocities interior to the solar circle, 9.9 kpc, can not be excluded (McClure-Griffiths et al. 2001; figure

4 and table 2). A possible association of the SNR with the surrounding HI shell (McClure-Griffiths et al. 2001; subsection 5.3.2 and figure 14) favors that the SNR is close to the absorbing HI clouds at  $4.9 \pm 0.3$  kpc (or at 9.9 kpc). It is worth noting that the line of sight of  $l = 330^\circ 2'$  intersects the Norma arm at distances of  $\simeq 6.3$  kpc and  $\simeq 11.3$  kpc (McClure-Griffiths et al. 2001; figure 14). Therefore, a reasonable distance upper limit to the SNR may be 11.3 kpc. Hereafter, we denote the SNR distance as  $d_{4.9}$  normalized to 4.9 kpc. For this distance and the radio shell's radius, the Sedov solution's age–radius relation gives a minimum age of  $t = 3.1 \times 10^3 (E_{51}/n_0)^{-1/2} d_{4.9}^{5/2}$  yr, with an explosion energy normalized to  $10^{51}$  erg and the interstellar medium density normalized to  $1 \text{ cm}^{-3}$ .

## 2. Observations

Observations of SNR G330.2+1.0 were performed with the ASCA (Tanaka et al. 1994) on 1999 September 11–12. ASCA had four X-ray telescopes that were equipped with two CCD cameras (SIS 0 and SIS 1) and two imaging gas-scintillation proportional counters (GIS 2 and GIS 3) (Ohashi et al. 1996; Makishima et al. 1996). The SIS was operated in the 1 CCD mode and its field of view ( $11' \times 11'$ ) did not cover the full spatial extent of the SNR shell. We therefore concentrated on the GIS data, which has a larger field of view ( $50'$  diameter) and a higher detection efficiency for hard X-ray sources. The effective exposure time for each GIS was 19.6 ks.

**Table 1.** Spectral parameters.

Object	Model	Photon Index/kT	Abund
G330.2+1.0	power-law	2.82 (2.61–3.04)	—
G330.2+1.0	mekal	2.99 (2.53–3.50)	< 0.5
AX J1601–5143	power-law	2.63 (2.47–2.82)	—
AX J1601–5143	mekal	3.32 (2.91–3.85)	0.14(0.02)

\* Unabsorbed 0.7–10 keV flux in  $\text{ergs}^{-1} \text{cm}^{-2}$ .

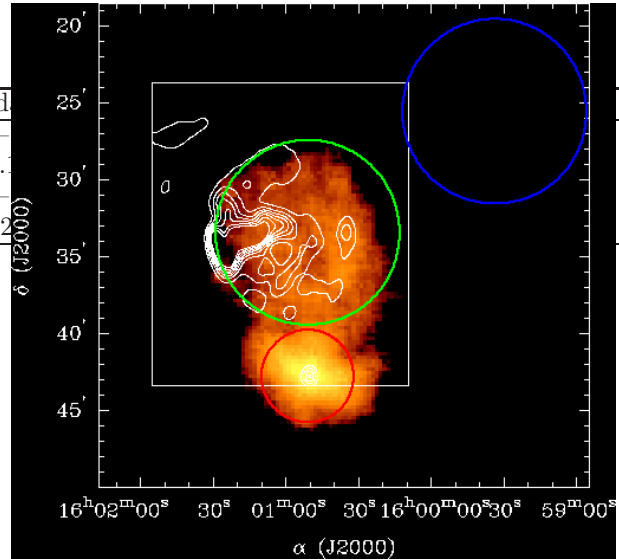
### 3. Analysis and Results

Figure 1 shows an X-ray image of G330.2+1.0 obtained with the GIS. An extended shell is clearly detected as well as a compact source in the south. The position of the compact source, as determined from the GIS image, is (16:00:51.0,  $-51:42:33$ )(J2000) (hereafter AX J1601–5143) with a possible error of a few arcminutes. The radial profile of the compact source is found to be consistent with a point source. Excluding background, the GIS count rate for AX J1601–5143 was 0.094 cps and 0.074 cps for GIS 2 and GIS 3, respectively. The lightcurve of AX J1601–5143 does not show any significant flux variability from timescales of minutes to hours. We did not detect any coherent pulsations either up to the Nyquist frequency of 128 Hz. Figure 2 shows the GIS image overlaid on the radio map. The radio emission is brightest at the eastern shell (toward the lower galactic latitude), while the X-ray emission is brighter in the western part. The surface brightness of the shell is clearly anti-correlated between the radio and X-ray bands.

Figures 2a and 2b show the GIS spectra for the SNR shell and the compact source, respectively, fitted with a power-law function modified by the interstellar absorption. As shown in figure 1, circular regions of 6' and 3' radii, centered at (16:00:50.9,  $-51:33:27$ )(J2000) and (16:00:50.9,  $-51:42:47$ )(J2000), were used to extract spectra for the SNR and the compact source, respectively. Background spectra were extracted from a circular region of 7.5' radius centered at (15:59:33.7,  $-51:25:35$ )(J2000). Spectral fits to a non-thermal (power-law) model and thermal (mekal) model by using XSPEC (Arnaud, 1996) are summarized in table 1. We further tried to investigate the spatial variation of the X-ray spectra across the SNR shell, but limited statistics did not allow us to find any significant variation.

### 4. Discussion

Since the absorption columns to G330.2+1.0 and AX J1601–5143 (table 1) do not exclude a possibility that they are at a similar distance, we explore if the two objects are physically associated or not. AX J1601–5143 is probably the same object as 1RXS J160045.0–514307 in the ROSAT all-sky survey faint source catalog (Voges et al. 2000). The cataloged position is 65'' from the GIS position. The PSPC countrate,  $0.032 \pm 0.012$  cps, is as expected from the GIS spectral parameters with either the



**Fig. 1.** X-ray image of the SNR shown by half tone. The contours show the radio map observed with the MOST (Whiteoak, Green 1996). The southern, middle, and northern circles show the regions from which the X-ray spectra of AX J1601–5143, G330.2+1.0, and the background, respectively, were extracted.

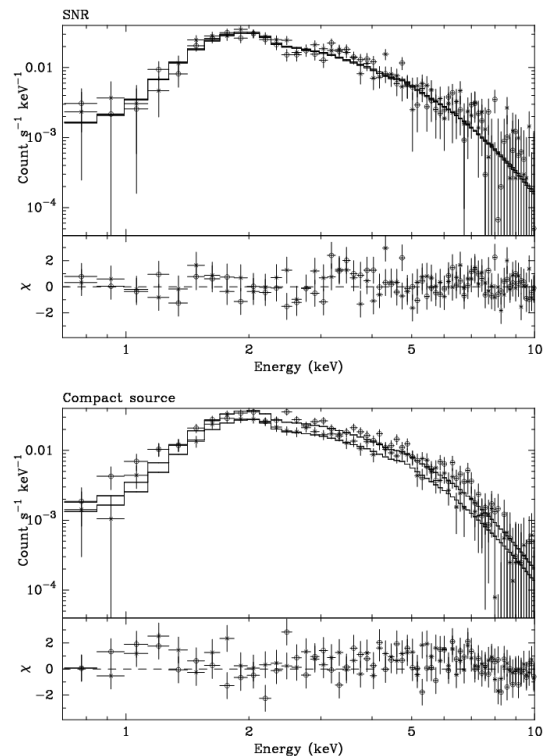


**Fig. 2.** X-ray spectra for the SNR and the compact source shown with the best-fit power-law function modified by the absorption. The circles and crosses show GIS 2 and GIS 3 data points, respectively.

mekal model or the power-law model, taking into account the statistical uncertainties of the PSPC and GIS data.

If the power-law model is appropriate, AX J1601–5143 could be a Crab-like object or a background active galactic nucleus. The absence of any significant long-term flux variability favors the former interpretation, but the required transverse velocity,  $v_t = 3.9 \times 10^3 (t_{\text{age}}[\text{yr}]/3100)^{-1} d_{4.9} \text{ kms}^{-1}$ , for the projected angular distance from the shell center,  $\simeq 8'.8$  or  $13 d_{4.9} \text{ pc}$ , is unreasonably large. Also, the observed photon index, 2.63, is steeper than any object powered by an energetic pulsar (e.g., Gotthelf 2003). Thus, it is unlikely that AX J1601–5143 is a Crab-like pulsar/nebula.

If the thermal interpretation is correct, AX J1601–5143 could be a nearby ( $d < 4.9 \text{ kpc}$ ) white dwarf binary with  $L_X < 5.5 \times 10^{34} d_{4.9}^2 \text{ ergs}^{-1}$ . We have not found any clear evidence of line emissions in the GIS spectra, and derive an equivalent width upper limit of  $EW < 400 \text{ eV}$  for a narrow line at 6.7 keV from helium-like iron. This equivalent width and the elemental abundance (table 1) are not inconsistent with the characteristics found in white-dwarf binaries (e.g., Ezuka, Ishida 1999). The remnant is in the crowded galactic plane, and it is not surprising that a point-like source has been found within the same field of view. We therefore conclude that G330.2+1.0 and AX J1601–5143 are not physically associated, and that G330.2+1.0 is a shell-type SNR without an energetic pulsar.

From a statistical point of view alone, we can not distinguish the better spectral model for the SNR shell (table 1). If the thermal model is appropriate, the relatively high temperature ( $kT = 2.99 \text{ keV}$ ) suggests that the SNR is young and emission lines from metal-rich ejecta should be expected. The absence of significant Mg, Si, S, and Fe K shell lines is incompatible with our knowledge for young, high-temperature SNRs, such as Cas-A, Tycho's, or Kepler's (e.g., Tsunemi et al. 1986; Kinugasa et al. 1999). The suppression of emission lines could occur if the interstellar medium density is very low, resulting in the low ionization state. This is unlikely, since the clumpy radio morphology suggests shock interaction with the dense medium. Therefore, it is difficult to explain the spectrum in the thermal model. We thus conclude that the most reasonable interpretation for the featureless spectrum in G330.2+1.0 is synchrotron radiation from relativistic electrons accelerated in the SNR shell.

To evaluate multi-wavelength emission, we fit the SNR spectrum with the `srcut` model, which describes synchrotron radiation from a power-law distribution of electrons with an exponential cut-off (Reynolds, Keohane 1999). For a fixed radio spectral index ( $\alpha = 0.3$ ) and flux density (5 Jy at 1 GHz) (Green 2004), the fit is significantly worse ( $\chi^2/\text{dof} = 470.6/392$ ) than that of the simple power-law model. This means that the radio and X-ray emission can not have originated from a simple, single population of electrons in a uniform magnetic field. The best-fit parameters are the break frequency of  $\nu_b = 4.3 \times 10^{15} \text{ Hz}$  and the absorption column of  $n_H = 5.1 \times 10^{22} \text{ cm}^{-2}$ . If the radio flux density

is considered as a free parameter, the fit becomes better ( $\chi^2/\text{dof} = 470.6/392$ ) with  $\nu_b = 7.0 \times 10^{16} \text{ Hz}$ , a flux density of  $S = 7.3 \times 10^{-3} \text{ Jy}$ , and  $n_H = 2.2 \times 10^{22} \text{ cm}^{-2}$ . The break frequency corresponds to an electron energy of  $E_b = 30 \cdot (B_5)^{-1/2} \text{ TeV}$ . Here,  $B_5$ , is the magnetic field of the emitting region normalized to 5  $\mu\text{G}$ . The small best-fit flux density ( $7.3 \times 10^{-3} \text{ Jy}$  at 1 GHz) compared to that observed (5 Jy) suggests that there are at least two populations of particles, and only a tiny fraction of the radio-emitting particles has an extended tail toward the TeV region.

As can be seen in figure 1, the surface brightness of the X-ray emission is anti-correlated with the radio emission. The X-ray emission is strongest at the western shell, where the lower radio intensity toward the higher galactic latitude suggests a lower ISM density. It is likely that moderately accelerated (GeV) electrons are efficiently decelerated in the eastern shell interacting with the dense ISM. In contrast, the lower ISM density in the western shell results in efficient acceleration to the TeV range. The co-existence of two distinct (radio bright/X-ray faint and radio faint/X-ray bright) shells in a single supernova remnant gives us an interesting opportunity to study the acceleration mechanisms in different ISM environments.

Interestingly, the X-ray luminosity of the shell,  $L_{\text{SNR}} = 4.6 \times 10^{34} d_{4.9}^2 \text{ ergs}^{-1}$  (0.7–10 keV) is comparable to that for RX J1713.7–3946 ( $1 \times 10^{35} d_1^2$ ), SN 1006 ( $\simeq 2 \times 10^{35} d_{2.2}^2 \text{ ergs}^{-1}$ ), RX J0852.0–4622 ( $2 \times 10^{34} d_1^2 \text{ ergs}^{-1}$ ) (Slane et al. 1999; Slane et al. 2001), within a factor of  $\simeq 5$ . There may be common physics at work for tuning the acceleration efficiency in these SNRs.

In summary, we reported on the discovery of a featureless X-ray spectrum in the SNR G330.2+1.0. We interpret this emission as coming from synchrotron radiation of electrons accelerated at the SNR shock as seen in SN 1006 and RX J1713.7–3946. Our preliminary analysis of the archived XMM-Newton data with short exposure ( $\sim 9 \text{ ks}$ ) qualitatively confirmed our findings presented herein. Further analysis of the XMM-Newton data with an emphasis on the nature of AX J1601–5143 will be presented elsewhere. Since the surface brightness of the shell is low, X-ray observations with Suzaku, which has a large effective area and low background, will be useful for an accurate determination of the SNR spectrum. Although neither G330.2+1.0 nor the compact source was detected in the recent H.E.S.S. survey (Aharonian et al. 2006), additional deep searches for TeV emission may be useful. For constraining different radiation mechanisms (inverse Compton effect, pion decay, non-thermal bremsstrahlung) in the TeV region, radio observations of the environmental molecular gas (e.g., Fukui et al. 2001) will be of great help.

The authors are grateful to the referee, P. Slane, for valuable suggestions that greatly improved the original draft.

This work is partly supported by a Grant-in-Aid for

Scientific Research by the Ministry of Education, Culture, Sports, Science and Technology (16002004). This work was financially supported by the Japanese Ministry of Education and the 21st Century COE Program named "Towards a New Basic Science: Depth and Synthesis".

## References

- Aharonian, F.A., et al. 2004, *Nature*, 432, 75  
Aharonian, F., et al. 2005, *A&A*, 437, L7  
Aharonian, F., et al. 2006, *ApJ*, 636, 777  
Arnaud, K.A. 1996, in *ASP Conf. Ser.*, 101, ed. G.H. Jacoby & J. Barnes (San Francisco: ASP), 17  
Caswell, J.L., Haynes, R.F., Milne, D.K., & Wellington, K.J. 1983, *MNRAS*, 1983, 915  
Ezuka, H., & Ishida, M. 1999, *ApJS*, 120, 277  
Fukui, Y., et al. 2003, *PASJ*, 55, L61  
Gotthelf, E.V. 2003, *ApJ*, 591, 361  
Green, D.A. 2004, *Bull. Astron. Soc. India*, 32, 335  
Kinugasa, K., & Tsunemi, H. 1999, *PASJ*, 51, 239  
Koyama, K., Kinugasa, K., Matsuzaki, K., Nishiuchi, M., Sugizaki, M., Torii, K., Yamauchi, S., & Aschenbach, B. 1997, *PASJ*, 49, L7  
Koyama, K., Petre, R., Gotthelf, E. V., Hwang, U., Matsuura, M., Ozaki, M., & Holt, S.S. 1995, *Nature*, 378, 255  
Makishima, K., et al. 1996, *PASJ*, 48, 171  
McClure-Griffiths, N.M., Green, A.J., Dickey, J.M., Gaensler, B.M., Haynes, R.F., & Wieringa, M.H. 2001, *ApJ*, 551, 394  
Muraishi, H., et al. 2000, *A&A*, 354, L57  
Ohashi, T., et al. 1996, *PASJ*, 48, 157  
Reynolds, S.P., & Keohane, J.W. 1999, *ApJ*, 525, 368  
Slane, P., Gaensler, B.M., Dame, T.M., Hughes, J.P., Plucinsky, P.P., & Green, A. 1999, *ApJ*, 525, 357  
Slane, P., Hughes, J.P., Edgar, R.J., Plucinsky, P.P., Miyata, E., Tsunemi, H., & Aschenbach, B. 2001, *ApJ*, 548, 814  
Tanaka, Y., Inoue, H., & Holt, S.S. 1994, *PASJ*, 46, L37  
Tsunemi, H., Yamashita, K., Masai, K., Hayakawa, S., & Koyama, K. 1986, *PASJ*, 306, 248  
Voges, W., et al. 2000, *IAUC*, 7432  
Whiteoak, J.B.Z., & Green, A.J. 1996, *A&AS*, 118, 329